

Internal and free energy in a pair of like-charged colloids: Monte Carlo simulations

Alejandro Cuetos,^{1,a)} Juan A. Anta,¹ and Antonio M. Puertas²¹*Departamento de Sistemas Físicos, Químicos y Naturales, Universidad Pablo de Olavide, 41013 Seville, Spain*²*Departamento de Física Aplicada, Universidad de Almería, 04120 Almería, Spain*

(Received 16 September 2010; accepted 1 October 2010; published online 20 October 2010)

The effective interaction between two colloidal particles in a bath of monovalent co- and counterions is studied by means of lattice Monte Carlo simulations with the primitive model. The internal electrostatic energy as a function of the colloid distance is studied fixing the position of the colloids. The free energy of the whole system is obtained introducing a bias parabolic potential, that allows us to sample efficiently small separations between the colloidal particles. For small charges, both the internal and free energy increase when the colloids approach each other, resulting in an effective repulsion driven by the electrostatic repulsion. When the colloidal charge is large enough, on the other hand, the colloid-ion coupling is strong enough to form double layers. The internal energy in this case decreases upon approaching the colloids because more ions enter the double layer. This attractive contribution to the interaction between the colloids is stronger for larger charges and larger ionic concentrations. However, the total free energy increases due to the loss of ionic entropy, and resulting finally in a repulsive interaction potential driven by the entropic contributions. The loss of ionic entropy can be almost quantitatively reproduced with the ideal contribution, the same level of approximation as the Derjaguin–Landau–Verwey–Overbeek (DLVO) theory. The overall behavior is captured by the DLVO theory qualitatively, and a comparison is made with the functional form predicted by the theory, showing moderate agreement. © 2010 American Institute of Physics. [doi:10.1063/1.3505148]

I. INTRODUCTION

Charges in soft matter are ubiquitous and control many fundamental and practical processes, ranging, e.g., from the transport in cell membrane to particle adhesion or coatings. Different from isolated charges, in soft matter a (typically polar) solvent is present with an electrolyte solution; a strong coupling due to electrostatic attraction is often observed, which also screens the charges and makes the interaction short ranged.¹ In general, the theoretical description of this problem is very complicated. The huge number of degrees of freedoms involved and the intrinsic long range character of the electrostatic interactions make necessary to implement very strong approximations. Hence, there are still many open questions about the thermodynamic and structural behavior of macroion solutions. The simple case of a charged sphere immersed in a solvent with an electrolyte solution was tackled more than 60 years ago by Derjaguin and Landau, and Verwey and Overbeek,² solving the Poisson–Boltzmann (PB) equation for the reduced electric potential ψ ,

$$\text{div grad } \psi = \kappa^2 \sinh \psi, \quad (1)$$

where κ is the inverse Debye length,

$$\kappa^2 = \frac{4\pi e^2}{\epsilon k_B T} \sum \rho_i z_i^2, \quad (2)$$

with e the elementary charge, ϵ the medium dielectric constant, k_B the Boltzmann constant, T the temperature, and z_i and ρ_i the ion valence and the ion density, respectively.

The model is further simplified by restricting to low potentials, so that $\sinh \psi \approx \psi$. In spherical coordinates this linearized equation gives the screened Coulombic (Yukawa) form for the electric potential. As derived by Derjaguin and Landau, the interaction between colloidal spheres is calculated using the electric potential between infinite planes; a decreasing exponential. The effective interaction between them is given by the increase in the free energy of the system upon approaching the planes from infinite to distance r , and the interaction between spheres is calculated by integrating in rings.^{3,4} In the limit of thick double layers (κr small) and in the linear superposition approximation, the interaction potential shows also a Yukawa-like form, with κ being the screening parameter.^{2,5} The Derjaguin–Landau–Verwey–Overbeek (DLVO) interaction potential can also be derived using density functional theory, giving the standard screened Coulombic interaction for fixed colloidal charges.^{6,7} The PB model is a mean field theory where it is assumed that the ionic distribution is dominated by the electrostatic potential, and ion-ion correlations are absent.⁸

Contrary to the expectations from this model, where similarly charged particles repel each other in the absence of other forces (such as Van der Waals), microscopy experi-

^{a)}Electronic mail: acuemen@upo.es.

ments both in the bulk⁹⁻¹¹ and under confinement^{12,13} showed attractions between like-charged colloids in a range of distances. Some of these experiments, however, have been criticized due to artifacts or irreproducibility,¹⁴ while more elaborated theoretical models have been developed.¹ It is now well understood that attractions can, in fact, appear due to charge inversion when the valency of the ions is high (or the colloid one sufficiently low)¹⁵⁻¹⁹ or due to steric effects.²⁰ These effects have been rationalized in terms of strong electrostatic coupling¹⁶ and ionic condensation.²¹ For ions with low valency, on the other hand, it is yet not clear whether attractions between like-charged colloids are real or an artifact, at least for aqueous suspensions at room temperature. For solvents with low dielectric constant, where the electrostatic coupling is stronger, attractions have been reported recently for monovalent counterions.²⁰

Because of computer limitations, simulations have not reached yet the colloidal limit, i.e., high colloidal charge and not-too-low salt concentrations (note that electroneutrality must be fulfilled and large colloidal charges imply a large number of counterions). In spite of this limitation, simulations with primitive models have shown attractions between like-charged colloids for multivalent counterions and strong electrostatic coupling.^{15-17,22} However, it is yet unclear whether attractions can indeed appear for higher colloidal charges, close to many experimental situations.

The objective of this work is to clarify these controversial issues. For this we have developed a new computer simulation strategy that makes it possible, contrary to previous reports, to compute the effective interaction between two charged colloidal particles with explicit consideration of the correlations (no mean field approximations), in the presence of salt ions, and for very large colloidal charges. This simulation technique is based in an extension of the umbrella sampling method.²³ This method allows us to calculate the effective interaction potential between two charged colloids and discriminate between the different contributions to the effective potential. With this method the effective potential could be calculated for large colloidal charges (up to 1000 times the elementary charge) in a reasonable computational time. The effect of the salt concentration also could be explored in a wide range. With the direct calculation of the effective potential between the colloids we can shed light upon the aspects commented above. We study whether, in the frame of the primitive model, attractions between like-charged colloids appear in nonconfined geometry. We also check the range of validity of the PB approximation and the standard DLVO theory at high colloidal charges, where it is expected to fail. We also have paid attention to the different contributions to the effective potential. For high charges, the double layers of the particles incorporate more and more ions when the particles approach each other. This results in a significant decrease of the internal energy, i.e., an attractive contribution to the free energy. However, the loss of the ionic entropy overcomes this energy gain, and the free energy is indeed repulsive, as the DLVO theory qualitatively predicts.

The paper is organized as follows. In Sec. II we intro-

duce the model and the computer simulation techniques. Results and discussion is presented in Sec. III. A summary and conclusions are presented in Sec. IV.

II. SIMULATION DETAILS AND METHODS

We have carried out Monte Carlo simulations at constant number of particles, volume, and temperature. The system consists of two positively charged colloidal particles of charge Ze (e is the charge unity) and diameter σ , N_s coions with charge e , and N_s+2Z counterions with charge $-e$. Note that with this number of particles global electroneutrality is ensured. The diameter of both co- and counterions is $\sigma/40$. The particles interact through the Coulomb potential; for two particles of species i and j (colloids and/or ions) the interaction is given by

$$\beta U_{ij}(r_{ij}) = \begin{cases} \infty & r_{ij} \leq \sigma_{ij} \\ \frac{Z_i Z_j}{r_{ij} \lambda_B} & r_{ij} \geq \sigma_{ij}, \end{cases} \quad (3)$$

where $\sigma_{ij}=0.5(\sigma_i+\sigma_j)$ is the contact distance between two particles. The Bjerrum length is set to $\lambda_B=\beta e^2/\epsilon=0.007\sigma$, and $\beta=1/k_B T$. This value of λ_B mimics the conditions of water at room temperature with colloids of $\sigma=100$ nm. Simulations were run in a rectangular box of dimensions $L_x \times L_y \times L_z$ with $L_x=25\sigma$, and $L_y=L_z=10\sigma$, giving a colloid volume fraction of 4×10^{-4} (snapshots of the system at different conditions are presented in Fig. 6 below). Periodic boundary conditions are applied in the three directions as usual.

The long range character of the Coulombic interactions is handled using the standard Ewald summation technique with conducting boundary conditions.²⁴ In the reciprocal space, only vectors with the modulus of the Fourier part of the Ewald sum bigger than 1×10^{-8} are considered in the summation. The real-space damping parameter α was fixed at $1.5\sigma^{-1}$. As the use of Ewald sums slows down the simulation, we have employed the technique proposed by Kumar and Panagiotopoulos²⁵ to speed up the calculations. In this method the positions of the particles are constrained to a discrete cubic lattice, with small lattice spacing, and the interaction energy between all pairs of lattice sites is calculated only once at the beginning of the simulation. The lattice parameter is defined as $\chi=\sigma/a$, with a the lattice spacing (the continuum limit is reached for $\chi \rightarrow \infty$). Hynninen *et al.*²⁶ have shown that, for charged colloids, the results obtained with this method are independent of χ if this parameter is large enough. We have used $\chi=35$ in all the simulations, close to the limit value found by Hynninen *et al.*²⁶

With this general characteristics we have carried out two types of simulations. In the first ones, the positions of the two colloidal particles were fixed at coordinates $(R/2, 0, 0)$ and $(-R/2, 0, 0)$, whereas ions were allowed to change their positions in the lattice according a standard Metropolis algorithm. The maximum displacement of the ions was fixed at 5σ . Starting from a random configuration, 5×10^5 Monte Carlo cycles were run to thermalize the system (a cycle consists of $2N_s+2Z$ trials to move one randomly chosen ion). 10^6 additional Monte Carlo cycles were run to obtain aver-

ages. With this method we have calculated the internal energy as a function of the intercolloidal distance $U(R)$ averaging the total electrostatic energy of the system, including colloid-colloid, colloid-ion, and ion-ion contributions.

Whereas this is useful to calculate the internal energy of the system, to calculate the interaction potential, however, the whole Hamiltonian of the system must be integrated in the phase space of the ions. The effective intercolloidal potential is given by the free energy as a function of the distance between them.^{2,7,27} The free energy can be obtained with the equation

$$F(R) - F_0 = -\frac{1}{k_B T} \log(P(R)), \quad (4)$$

where $F(R)$ is the free energy of the system with the two colloids at distance R , F_0 is an undetermined constant, and $P(R)$ is the probability to find the colloids at distance R . It could be possible to calculate the latter magnitude in a Monte Carlo simulation where the colloids were movable, similar to the experimental determination from the radial distribution function.²⁸ In this method, however, the regions with strong repulsion are poorly sampled, requiring extremely long simulations. To surmount this difficulty, we have performed umbrella sampling Monte Carlo simulations. The umbrella method has been widely used in simulations of rare events.^{23,24,29,30} It consists in the introduction of a bias potential that favors configurations that are rarely visited. The effect of this bias potential over the probability distribution is removed at the end of the simulation. Therefore, we have run simulations where the two colloidal particles can move and a bias potential that depends on R according to

$$U_{\text{bias}} = K(R - R_0)^2, \quad (5)$$

where K gives the strength of the bias potential and R_0 is a distance of reference. Changing K and R_0 allows us to calculate $P(R)$ in a particular range of distances.

The simulation method is implemented as follows. 2.5×10^5 Monte Carlo cycles have been run to equilibrate the system and 10^6 cycles to obtain averages. One Monte Carlo cycle comprises a trial to move each colloid in any direction plus $2N_s + 2Z$ trials to move an ion chosen at random. As a Monte Carlo move of one colloid will have a high probability to be rejected due to overlaps with ions, we have used the swap move technique: ions that overlap with the new colloid position are moved into the space left empty by the displaced colloid.^{26,31} The acceptance ratio of moves per colloid was maintained at 40%, while the maximum displacement for microions was fixed at 5σ . The Monte Carlo moves described here are done with the interparticle potential described in Eq. (3), without the influence of the bias potential, equation (5). This bias potential is only applied after the end of the each Monte Carlo cycle, accepting or rejecting all the cycle according to the Metropolis rule.

Figure 1 exemplifies how the free energy is obtained. A given pair of values for K and R_0 allows us to sample $P(R)$ in a range of R , as shown in the upper panel. For this K and R_0 , the free energy can be calculated with Eq. (4) and removing the effect of the bias potential, except for the undetermined constant F_0 (which is set to zero in the intermediate panel).

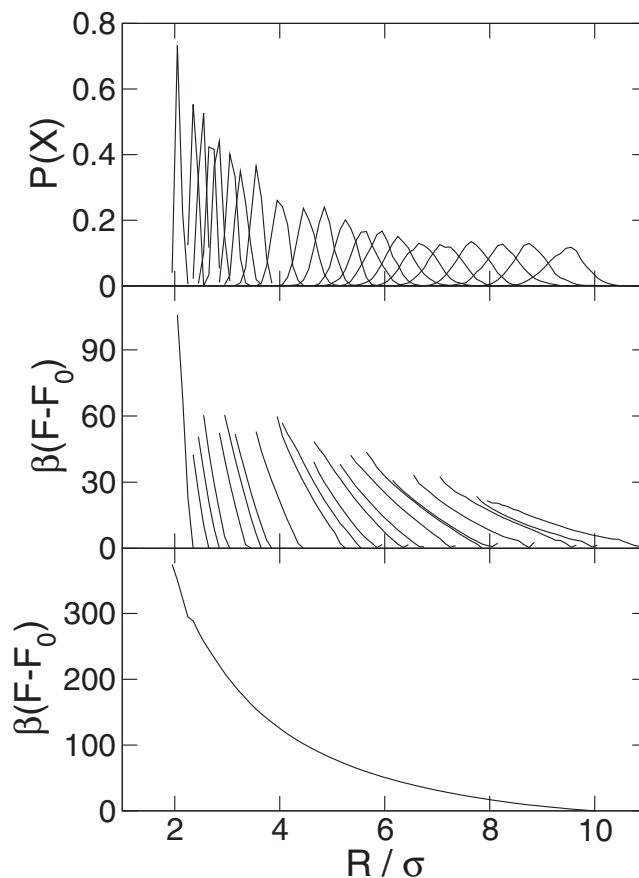


FIG. 1. Example of the calculation of the free energy of the system ($Z = 500$ and $N_s = 500$) as a function of the colloidal distance R . The top panel shows the biased density probability $P(R)$ for different values of K and R_0 from $K=2.5$ and $R_0=8\sigma$ (rightmost curve) to $K=100$ and $R_0=0$ (leftmost curve). The intermediate panel shows the free energy for every pair of K and R_0 , with $F_0=0$, and the bottom one the total free energy with all traces connected and $F(R=10\sigma)=0$.

Fixing $F(R=10\sigma)=0$ arbitrarily, instead of the standard $F(R \rightarrow \infty) \rightarrow 0$, we set the value of F_0 for the simulation where $R=10$ has been visited. The value of F_0 for all other simulations is then calculated forcing that the free energy must be continuous, i.e., minimizing the difference in F from two simulations where the $P(R)$'s overlap. The final result is presented in the lower panel of Fig. 1. In this work, the value of K has been varied between 0.5 and 100 and R_0 between 0 and 8σ .

III. RESULTS AND DISCUSSION

The electrostatic internal energy of the system is calculated by fixing the position of the two colloidal particles and equilibrating the configuration of ions with standard Monte Carlo moves. Results without added pairs (only counterions are present) are shown in Fig. 2 for different colloidal charges. In all cases the internal energy when the colloid separation is $R=10\sigma$ is subtracted. Note that this makes the internal energy to be arbitrarily zero at $R=10\sigma$. For low and moderate charges, the internal energy increases upon approaching the colloidal particles, as expected for two positively charged spheres. However, when the colloidal charge is large the internal energy becomes counterintuitively negative and continues to decrease for bigger charges. The inter-

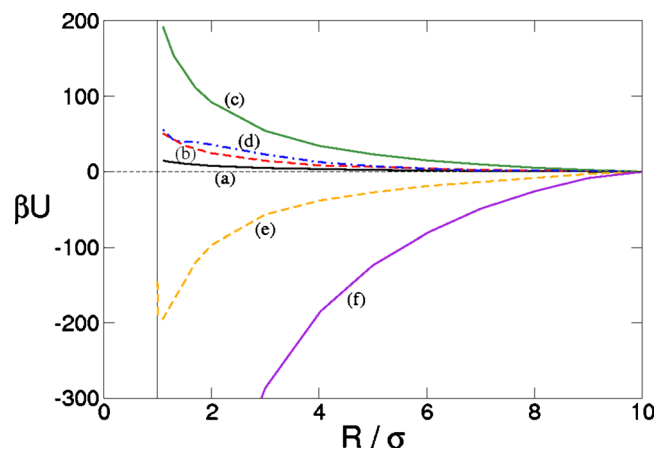


FIG. 2. Internal energy of the system with the two colloidal particles fixed at a separation distance R , with no salt added, for colloidal charge (a) $Z=50$, (b) 100, (c) 200, (d) 500, (e) 600, and (f) 1000. Note that upon increasing the charge, the internal energy first is positive and increases, but above $Z \sim 200$ decreases and becomes negative.

nal energy is maximal for charges around $Z=200$ and is constant for $Z \approx 515$. Note that the upturn of the internal energy at small separation for $Z=600$ (observable also at all other charges) is due to the electrostatic repulsion between the highly charged colloids which cannot be screened by the ionic clouds at this short distance. It is important to note that because the valence of the ions is small, ionic condensation can be ruled out.

Additional ionic pairs in the system are expected to screen the electrostatic interaction between the colloids. This is indeed the case for $Z=50$, as shown in Fig. 3 (upper panel), where the increase of the internal energy moves to shorter distances as more salt is added. Contrary to this expectation, for $Z=500$ the internal energy becomes negative and increases in absolute value with increasing salt concentration. Thus, for a particular number of ionic pairs, the internal energy is almost constant in a wide range of distances between the colloidal particles. In all cases, the upturn at short distances mentioned above is again observed, although it is more evident when the internal energy is negative.

We have shown in the two figures above that the internal energy of the whole system increases when the colloidal particles approach each other only for low charges and low salt concentration. On the other hand, U decreases when the charge or the salt concentration is large enough. Our present results indicate that this trend does not saturate with the colloidal charge or the ionic pairs. However, it must be stressed here that the effective interaction potential between the colloidal particles is not given by the internal energy, but by the free energy of the whole system. In fact, when the two colloidal particles are free to move in the simulations, they separate from each other for all charges and salt concentrations. Therefore, Figs. 2 and 3 are not indicative of like-charge attraction in colloidal systems, although a strong repulsive contribution is needed to make up for the decrease of the internal energy so that a net repulsive interaction is obtained. The free energy of the system is shown in Fig. 4 for different colloid charges without added salt (upper panel) and $Z=500$ with different amounts of ion pairs (lower panel).

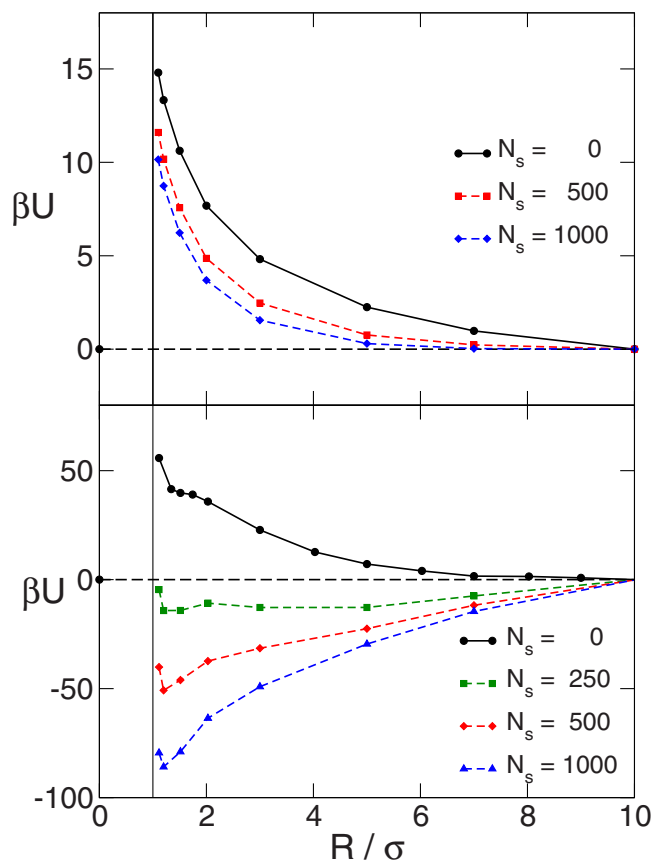


FIG. 3. Internal energy of the system as a function of the colloidal separation, for $Z=50$ (upper panel) and $Z=500$ (lower panel) and different numbers of coion-counterion pairs (N_s), as labeled. Note that for $Z=500$ the internal energy becomes negative upon adding salt.

The free energy is obtained from umbrella sampling of the system with an external parabolic potential, as described in Sec. II.

As expected for like-charged colloids, the free energy increases upon approaching the colloidal particles, indicating a repulsive interaction at all the charges and salt concentrations studied here. The free energy increases monotonously with the colloidal charge, showing that the repulsion is stronger and stronger. On the other hand, adding ion pairs to the system screens the repulsion, reducing its range, as one would expect. Our simulations, therefore, show no signature of attractions between similarly charged colloids.

The change from the decreasing trend of the internal energy to the increasing free energy must have its origin in the entropy of the system S and particularly that of the ions. S , calculated from $F=U-TS$, is plotted in Fig. 5 for the same charges and salt concentrations as Fig. 4. Upon approaching the colloidal particles, the entropy decreases in all cases. For $Z=50$ the decrease of entropy adds to the increasing internal energy and both of them contribute to the repulsive interaction potential. For $Z=500$, on the other hand, the decrease of entropy is much larger than for $Z=50$ (note the different y-scales in both panels) and induces a strong increase of the free energy. This competes with the gain in the internal (electrostatic) energy, resulting finally in the repulsive interaction shown in Fig. 4. Introducing ion pairs in the medium modi-

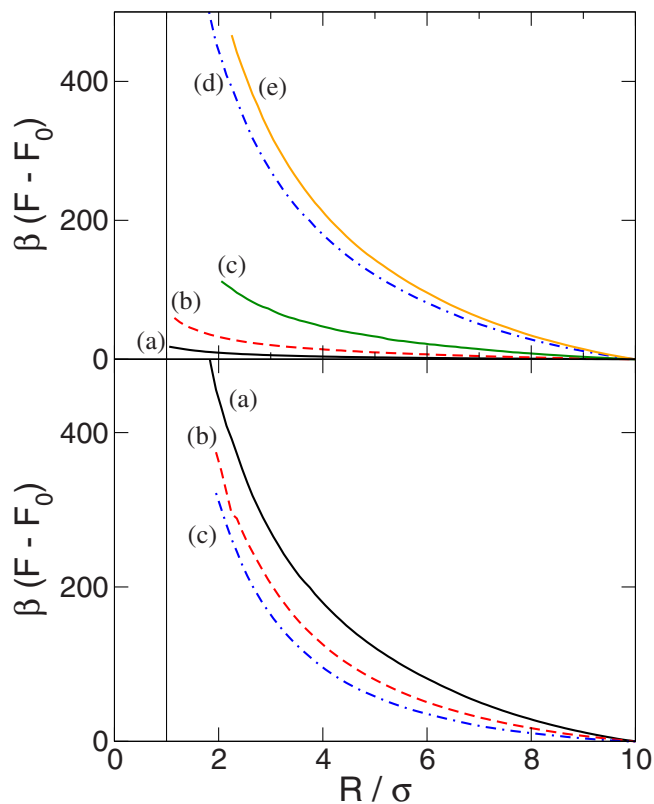


FIG. 4. Free energy of the system as a function of the colloidal separation. In the upper panel, different values of the colloidal charge without added salt are studied: (a) $Z=50$, (b) $Z=100$, (c) $Z=200$, (d) $Z=500$, and (e) $Z=600$. In the lower one, $Z=500$ is studied and the different numbers of ion pairs (a) $N_s=0$, (b) 500, and (c) 1000 are considered.

fies only quantitatively the decrease of entropy; for $Z=50$, S decreases slightly with the number of ion pairs, whereas a small increase is observed for $Z=500$.

The decrease in entropy must be caused by the structuring of the ions upon approaching the colloidal particles. Furthermore, since the decrease is stronger for larger charges, the ion structuring must be caused by the large colloidal charges, i.e., the ionic clouds around the colloids. This can be directly observed by studying the local density of ions in the system for large Z , where the effect is more dramatic. In Fig. 6 we plot the local charge density in the cylinder centered in the X -axis (the line that contains the centers of the colloidal particles), of radius $\sigma/2$, for the deionized system and $N_s=500$. These results are obtained from canonical simulations with the colloids fixed at a given distance.

When the particles are well separated, the ionic clouds around the colloidal particles are symmetric, but when the colloidal particles approach each other, the counterions concentrate in the region between the colloids raising the local charge density. Far away from the colloids, the density of counter- and coions (not shown) is almost similar, and the local charge decays to zero. Two snapshots are included in the figure for large and small separations. The same phenomenology is observed for both the deionized system and when salt is added. This figure demonstrates that the decrease of entropy is caused by the increasing concentration of ions in a particular spatial region. To obtain an additional confirmation of this argument, we have calculated the theoretical contri-

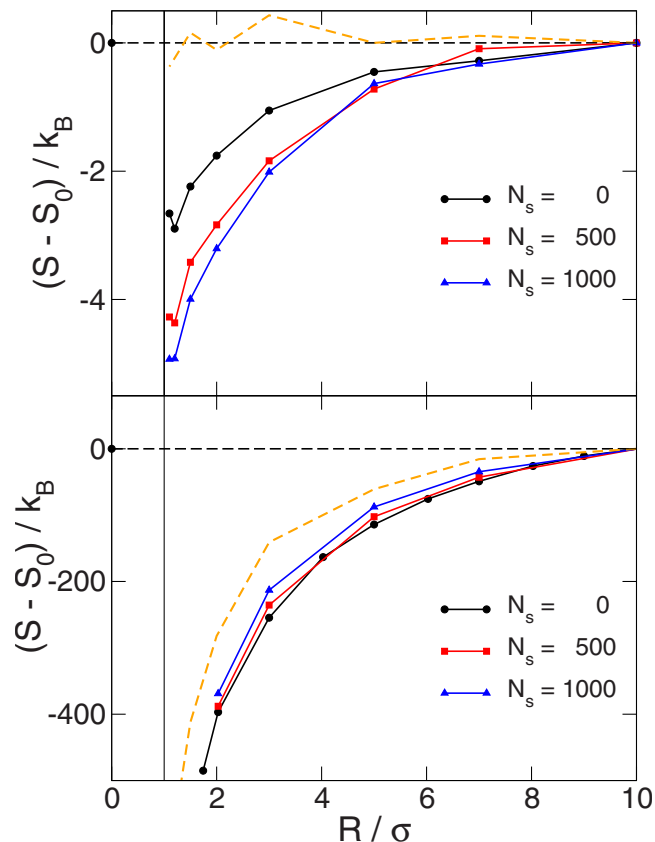


FIG. 5. Entropy of the system calculated from $F=U-TS$ for $Z=50$ (upper panel) and $Z=500$ (lower panel), and the same amounts of ion pairs as Fig. 3, as labeled. In both panels dashed lines correspond to the ideal contribution of the entropy for the deionized term calculated by Eq. (6).

bution of the inhomogeneity in the counterion distribution. We assume that this contribution corresponds to the entropy of an ideal gas of inhomogeneously distributed particles,³²⁻³⁴ i.e.,

$$S_{id} = -k_B \int d^3\mathbf{r} \rho_c(\mathbf{r}) (\ln[4\pi\Lambda^3 \rho_c(\mathbf{r})] - 1), \quad (6)$$

where Λ is the thermal de Broglie wavelength and $\rho_c(\mathbf{r})$ is the local ionic density at point \mathbf{r} , measured in the simulations. In Fig. 5 we have represented this theoretical (ideal) contribution of the entropy of the counterions for colloidal charge $Z=50$ and $Z=500$, in both cases without added salt. It can be observed that for $Z=50$ the ideal contribution is smaller than the statistical noise. On the contrary, for $Z=500$ the ideal part is the main contribution to the entropy, showing the same dependence with the colloidal distance that the global entropy, and almost quantitative agreement. Hence, we can conclude that the main contribution to the increase of the entropy when two colloids approach at high colloidal charge is a purely ideal contribution that comes from the confinement of the counterions in small volumes around the colloids, i.e., the structure of the double layer. The deviation of the simulated entropies from the prediction of Eq. (6) comes from the contribution of the correlation between ions. In our simulations we observe that this contribution is relatively small even for high colloidal charges.

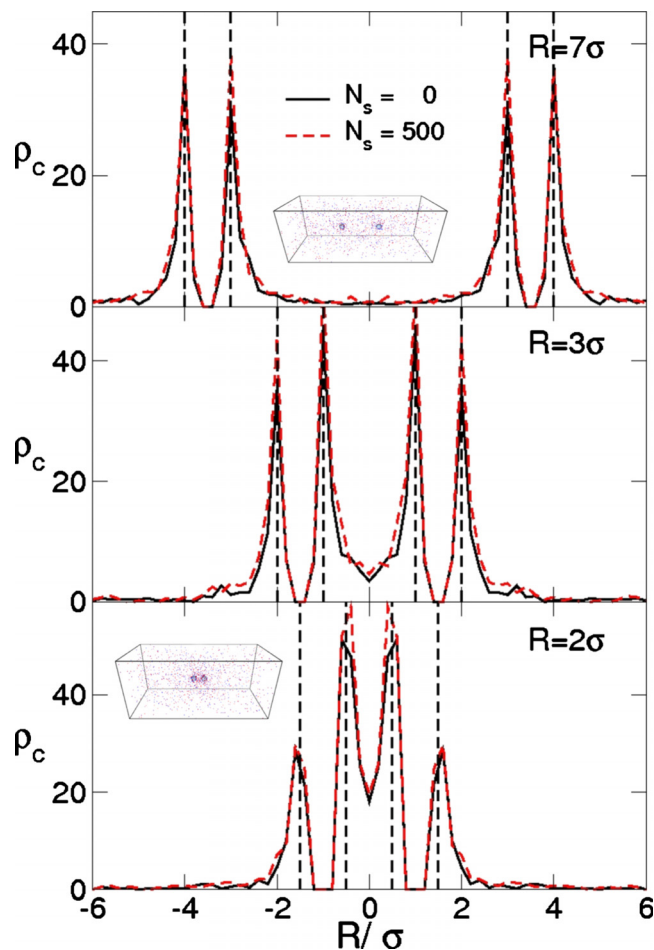


FIG. 6. Number concentration of counterions in the cylinder of radius $\sigma/2$ that contains both colloidal particles. As labeled, the salt-free and $N_s=500$ cases are studied, for $Z=500$, at different particle separations. The vertical dashed lines show the position of the particles. Snapshots for $X_0=7$ and $X_0=2$ with $N_s=500$ are also included (ions are represented with diameter $\sigma/10$ to be visible).

Since the ions group around the colloidal particles more densely as the colloids approach each other, this effect can also be studied by monitoring the number of counterions in the electric double layer. The radial distribution functions of counterions around the isolated colloids are shown in the inset in Fig. 7 for $Z=500$ with different concentrations of added salt. Since the density of counterions has decayed almost to the bulk value at $\sim 1.5\sigma$, we take this value as the radius of the electric double layer (EDL); ions located at distances shorter than $R_{\text{EDL}}=1.5\sigma$ are then assumed to belong to the EDL. The number of counterions in the EDL is presented in Fig. 7 for different values of the colloid charge with $N_s=0$ (upper panel) and for $Z=500$ with different amounts of ion pairs (lower panel).

It is interesting to note that the isolated particles form EDL only for high charges ($Z \geq 200$). This corresponds to the charge where the colloid-counterion coupling is equal to the thermal energy (note that $\sigma/\lambda_B=142.86$). In this case, when the colloidal particles are held close to each other, more ions are forced into the region between them. The growth in the number of ions in the EDL is quite significant: from ~ 70 to ~ 145 for $Z=500$ and from ~ 120 to ~ 220 for $Z=600$, causing the important decrease of the internal energy and the total

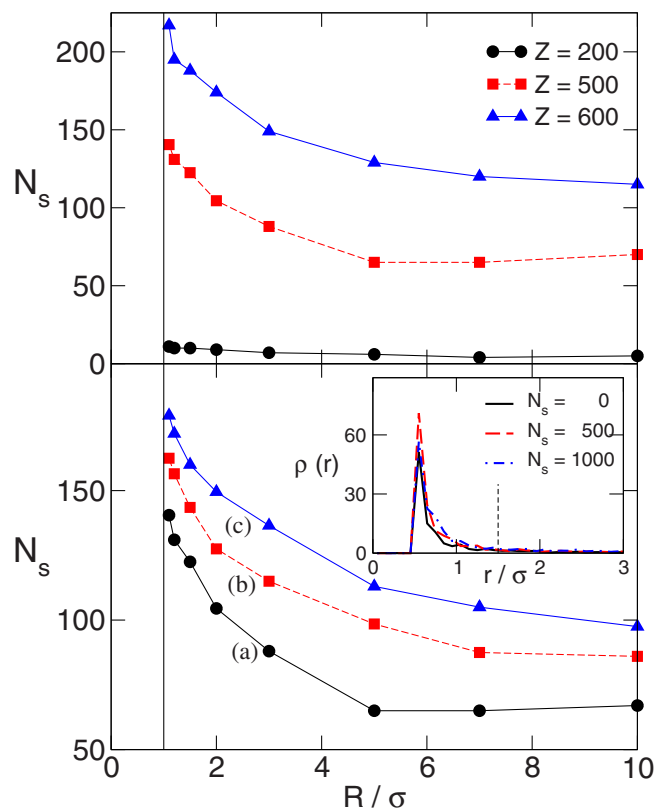


FIG. 7. Inset to lower panel: Radial distribution function of counterions around an isolated colloidal particle (obtained for large colloidal separation). The vertical dashed line shows the estimated radius of the double layer. Main panels: Number of counterions in the double layer of every colloidal particle as a function of the colloidal separation, for different colloid charges with $N_s=0$ (upper panel: Z increases from bottom to top) and $Z=500$ and different values of (a) $N_s=0$, (b) 500, and (c) 1000.

entropy discussed above. In the lower panel of Fig. 7, we show that this behavior persists when ion pairs are added to the system. For larger N_s , the EDL contains more counterions, pointing to the competition between electrostatics (forcing the counterions to the EDL) and entropy (driving the particles away from them).

The results here presented indicate that there is no attraction between like-charged colloids with monovalent ions, even for high colloidal charges. We have shown that this is a consequence of pure electrostatic repulsion (at low electrostatic coupling) and to the accumulation of ions and subsequent loss of entropy (at high electrostatic coupling). This is the same behavior predicted by the DLVO theory, at least at a qualitative level.⁴ Since the simulation provides a direct route to compute the internal energy, the entropy, and the free energy, it is interesting to compare the latter with the DLVO effective potential.

To see whether the simulated free energies reproduce the classical Yukawa-like functionality of the DLVO potential in the linear approximation, we have fitted the simulated data to the function

$$u(r) = A_0 \frac{e^{-A_1 R}}{R} - A_0 \frac{e^{-10A_1}}{10\sigma}, \quad (7)$$

where A_1 should theoretically correspond to the inverse Debye length of Eq. (2), whereas A_0 is related to an effective

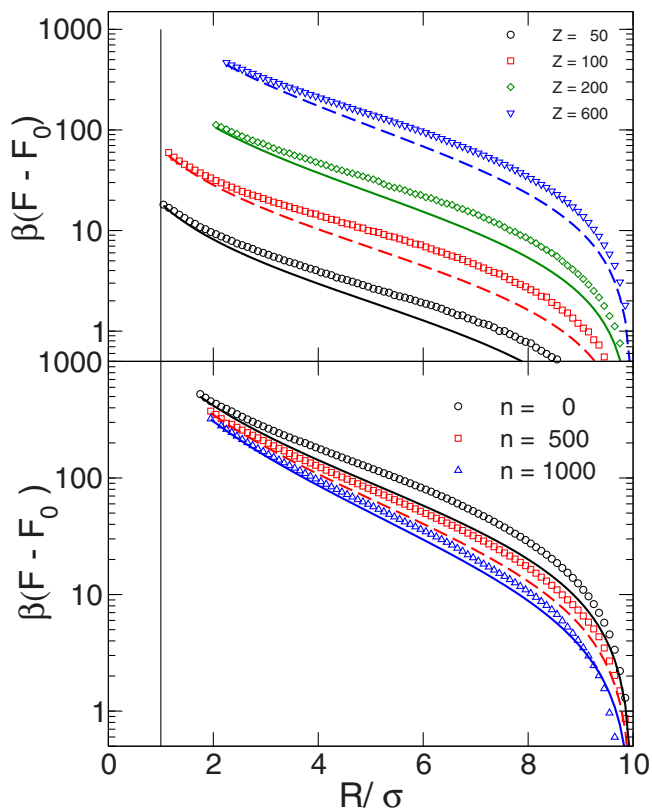


FIG. 8. Simulated free energies (symbols) and numerical fittings to Eq. (7) (lines) for different colloidal charges without added salt (upper panel) and for $Z=500$ and different values of N_s . Note that although the whole function is plotted, the fitting is restricted to the region of short and intermediate distances.

colloidal charge, which according to the DLVO theory (for spherical colloids at constant charge in the linear approximation) should be^{6,7,35}

$$A_0 = Z^{*2} e^2 / \epsilon, \quad Z^* = Z \frac{\exp[\kappa\sigma/2]}{1 + \kappa\sigma/2}. \quad (8)$$

In Fig. 8 we plot the simulated free energies and the result of the fitting to Eq. (7) in a log-linear scale. We must note that the second term in Eq. (7) is added in order to fulfill the same condition as the free energy from the simulations ($F(R=10\sigma)=0$). The fitting procedure is restricted to small and moderate distances to avoid spurious effects from this condition. Results of the best fitted parameters and the theoretical values are shown in Table I.

We observe that the simulation data reproduce a Yukawa-like functionality in all cases, at least at short and moderate distances. This result is consistent with the findings of Amico and Löwen³⁵ and Allahyarov and Löwen,³⁶ who also predict Yukawa-like interactions from molecular dynamics and Monte Carlo simulations. This is also consistent with the theoretical prediction about the validity of a mean field approximation, such as the PB theory, when the parameter $2\lambda_B^2 Z / \sigma^2$ is small.¹ In our case, the maximum value of this parameter is around 0.1.

The qualitative agreement between theory and simulation becomes almost quantitative at low colloidal charges and no salt, where the simulated free energies reproduce the theoretical DLVO values of the prefactor and the screening

TABLE I. Fitting parameters of the simulated free energies to Eq. (7) and theoretical values of Eqs. (2) and (8). The correlation index was above 0.99 in all cases. Top: results for different colloidal charges without added salt. Bottom: results for several values of N_s at colloidal charge $Z=500$.

Z	A_0	$A_1\sigma$	$\kappa\sigma$ [Eq. (2)]	A_0 [Eq. (8)]
50	21.1	0.066	0.060	17.5
100	73.3	0.065	0.085	70.1
200	297	0.116	0.120	280
500	1171	0.130	0.190	1764
600	1506	0.150	0.208	2545
N_s	A_0	$A_1\sigma$	$\kappa\sigma$ [Eq. (2)]	A_0 [Eq. (8)]
0	1161	0.126	0.190	1764
500	1072	0.194	0.269	1779
1000	1046	0.255	0.329	1793

parameter of Eqs. (2) and (8). This is explained by the fact that at conditions of weak electrostatic coupling, the linearization of the PB equation becomes more accurate. Hence, as the colloidal charge is increased, or more salt is added, the departure from the simple DLVO theory is augmented. However, the pure Yukawa functionality is maintained for all cases studied.

The failure of the simple DLVO potential at conditions of high colloidal charge can be due to either influence of correlations or breakdown of the linear approximation. However, the comparison of the ideal entropies with the simulation data indicates that correlations do not contribute significantly to the structure of the ions around the colloidal particles, which is what determines the colloid-colloid effective interactions. Hence the failure of the linear approximation (i.e., electrostatic potential much larger than the thermal energy) is the most likely cause of the departure from the theoretical DLVO potential. Nevertheless, the fact that the simple Yukawa functionality is maintained suggests that it is possible to find *renormalized* values of the screening length and the colloidal charge. As a matter of fact Belloni²¹ demonstrated that it is possible to keep the linearized version of the PB equation with a renormalized charge to achieve an accurate description of the colloid-colloid structure factor. The importance of this charge renormalization is controlled by the parameter $Z\lambda_B/\sigma$.³⁷ In our case this parameter changes from 1 to approximately 5, which is the limit where this effect starts to become relevant. In this work, our renormalized charges would be those extracted from Table I. Interestingly enough, the effective charges are smaller than the theoretical ones at high colloidal charges, as it could be expected from the usual renormalization procedures.²¹ It must be born in mind that the simulations show that the accumulation of ions in the vicinity of the colloidal surface is very strong at high colloidal charges, hence explaining the decrease of the effective charge.

IV. CONCLUSIONS

We have carried out Monte Carlo simulations of a system comprised of two colloids and monovalent co- and counterions interacting via a pure coulombic potential plus a hard-sphere interaction. Colloidal charges ranging from 50 to

1000 elementary charges have been studied as well as different concentrations of added salt. The simulation results have been used to obtain the internal free energy, the entropy, and the free energy as a function of the colloid-colloid distance. It is found that whereas the internal energy becomes attractive at high colloidal charges, the free energy (which corresponds to the true effective colloid-colloid interaction) remains repulsive in all cases. The analysis of the simulated entropies indicates that the origin of the repulsion is, at low colloidal charges, purely electrostatic, whereas at high charges, the repulsion arises from the loss of entropy that takes place when the colloids approach each other. In addition, the effective interaction is found to reproduce a Yukawa potential at both low and high electrostatic coupling, but the theoretical DLVO potential is reproduced quantitatively only at low colloidal charges and no salt. It should be stressed that this extreme conditions (low salt concentrations or high colloidal charge) are out of the conditions where the original DLVO theory applies. In any case, our results suggest that the Yukawa potential can be used to simulate charged colloids with very high charges and low salt concentration.

The good agreement between simulation results and theory indicates that no attraction is expected from the primitive model of colloids at least for monovalent ions in the bulk. It also highlights the good performance of the linearized PB theory, which works efficiently even for high colloidal charges provided a suitable renormalization of the bare charge is applied. Furthermore, the Monte Carlo method here devised, which includes an umbrella technique to compute the free energy with reasonable computer resources, proves to be an efficient tool to extract colloid-colloid effective interactions with colloidal charges of up to 1000 elementary charges. This opens the way to study colloidal stability in more cumbersome scenarios such as confined systems, multivalent ions, and suspensions in solvents of low dielectric constant. Work on this line is being carried out.

ACKNOWLEDGMENTS

This research has been funded by the Regional Government of Andalucía through Project Nos. P07-FQM-02595 and P09-FQM-4938.

- ¹ A. Naji, S. Jungblut, A. G. Moreira, and R. R. Netz, *Physica A* **352**, 131 (2005).
- ² E. J. W. Verwey and J. Th. G. Overbeek, *Theory of the Stability of Lyophobic Colloids* (Elsevier, Amsterdam, 1948).
- ³ J. Lyklema, *Fundamentals of Interface and Colloid Science* (Elsevier, Amsterdam, 2005).
- ⁴ J. Th. G. Overbeek, *Colloids Surf.* **51**, 61 (1990).
- ⁵ W. B. Russel, D. A. Saville, and W. R. Schowalter, *Colloidal Dispersions* (Cambridge University Press, Cambridge, 1989).
- ⁶ R. van Roij, *J. Phys.: Condens. Matter* **12**, 263 (2000).
- ⁷ R. van Roij, M. Dijkstra, and J.-P. Hansen, *Phys. Rev. E* **59**, 2010 (1999).
- ⁸ R. Messina, *J. Phys.: Condens. Matter* **21**, 113102 (2009).
- ⁹ B. V. R. Tata, P. S. Mohanty, and M. C. Valsakumar, *Solid State Commun.* **147**, 360 (2008).
- ¹⁰ I. Sogami and N. Ise, *J. Chem. Phys.* **81**, 6320 (1984).
- ¹¹ A. E. Larsen and D. G. Grier, *Nature (London)* **385**, 230 (1997).
- ¹² J. C. Crocker and D. G. Driver, *Phys. Rev. Lett.* **77**, 1897 (1996).
- ¹³ M. D. Carbajal Tinoco, F. Castro Román, and J. L. Aráuz Lara, *Phys. Rev. E* **53**, 3745 (1996).
- ¹⁴ J. Baumgartl, J. L. Arauz-Lara, and C. Bechinger, *Soft Matter* **2**, 631 (2006).
- ¹⁵ P. Linse and V. Lobaskin, *J. Chem. Phys.* **112**, 3917 (2000).
- ¹⁶ P. Linse, *J. Chem. Phys.* **113**, 4359 (2000).
- ¹⁷ J. Režičič and P. Linse, *J. Chem. Phys.* **114**, 10131 (2001).
- ¹⁸ J. A. Anta and S. Lago, *J. Chem. Phys.* **116**, 10514 (2002).
- ¹⁹ J. C. Butler, T. Angelini, J. X. Tang, and G. C. L. Wong, *Phys. Rev. Lett.* **91**, 028301 (2003).
- ²⁰ E. Allahyarov, E. Zaccarelli, F. Sciortino, P. Tartaglia, and H. Löwen, *Europhys. Lett.* **78**, 38002 (2007); **81**, 59901 (2008).
- ²¹ L. Belloni, *Colloids Surf., A* **140**, 227 (1998).
- ²² A. V. Brukhno, T. Åkesson, and B. Jönsson, *J. Phys. Chem. B* **113**, 6766 (2009).
- ²³ G. M. Torrie and J. P. Valleau, *J. Comput. Phys.* **23**, 187 (1977).
- ²⁴ D. Frenkel and B. Smit, *Understanding Molecular Simulation* (Academic, New York, 2002).
- ²⁵ A. Z. Panagiotopoulos and S. K. Kumar, *Phys. Rev. Lett.* **83**, 2981 (1999).
- ²⁶ A.-P. Hynninen and M. Dijkstra, *J. Chem. Phys.* **123**, 244902 (2005).
- ²⁷ J. A. Anta, *J. Phys.: Condens. Matter* **17**, 7935 (2005).
- ²⁸ G. M. Kepler and S. Fraden, *Phys. Rev. Lett.* **73**, 356 (1994).
- ²⁹ G. M. Torrie and J. P. Valleau, *Chem. Phys. Lett.* **28**, 578 (1974).
- ³⁰ S. Auer and D. Frenkel, *Nature (London)* **409**, 1020 (2001).
- ³¹ V. Lobaskin and K. Qamhieh, *J. Phys. Chem. B* **107**, 8022 (2003).
- ³² D. Chandler, *Introduction to Modern Statistical Mechanics* (Oxford University Press, Oxford, 1987).
- ³³ P. Tarazona and R. Evans, *Mol. Phys.* **52**, 847 (1984).
- ³⁴ P. V. Giaquinta and G. Giunta, *Physica A* **187**, 145 (1992).
- ³⁵ I. D'Amico and H. Löwen, *Physica A* **237**, 25 (1997).
- ³⁶ E. Allahyarov and H. Löwen, *J. Phys.: Condens. Matter* **21**, 424117 (2009).
- ³⁷ B. Zoetekouw and R. van Roij, *Phys. Rev. Lett.* **97**, 258302 (2006).